In Situ Raman Spectroscopy Study of Oxidation of Double- and Single-Wall Carbon Nanotubes

S. Osswald,[†] E. Flahaut,[‡] and Y. Gogotsi*,[†]

Materials Science and Engineering Department and A. J. Drexel Nanotechnology Institute, Drexel University, Philadelphia, Pennsylvania 19104, and Centre Interuniversitaire de Recherche et d'Ingénierie des Matériaux, UMR CNRS 5085, Université Paul Sabatier, 118 Route de Narbonne, 31062 Toulouse, France

Received December 13, 2005. Revised Manuscript Received January 16, 2006

In situ Raman spectroscopy allows for a detailed and time-resolved investigation of the kinetics of complex physical or chemical processes. Oxidation has become a frequently used method for the removal of disordered carbon species from carbon nanotubes. Oxidation, however, can also induce damage to the tubes and destroy most of the sample. We conducted an in situ Raman spectroscopy study of the oxidation of double- and single-walled carbon nanotubes (DWCNT and SWCNT) under isothermal and nonisothermal conditions to identify the temperature range in which the oxidation of amorphous carbon occurs without any changes with respect to the tubes and their structure. In situ Raman spectroscopy analysis of the oxidation of DWCNTs showed a decrease in the intensity of the D band starting around 370 °C, followed by complete D band elimination at 440 °C. Oxidation studies of SWCNTs showed a similar decrease in the D band intensity, but the D band was not completely eliminated. Furthermore, in situ measurements allow us to determine the different contributions to the D band feature and show the relationship between the D band, G band, and RBM Raman modes in the Raman spectra of DWCNT upon heating. Isothermal oxidation provides an efficient purification method for DWCNTs and SWCNTs, which is also selective to tube diameter. After oxidation, tubes show clean surfaces without disordered or amorphous carbon impurities.

Introduction

Single- and double-wall carbon nanotubes are the smallest members of the carbon nanotube family in terms of the number of walls. They have many attractive electronic and mechanical properties, but large amounts of tubes of high purity are required for precise measurement of properties and industrial applications of nanotubes. Several methods have been proposed for the synthesis of DWCNTs, such as catalytic chemical vapor deposition (CCVD),[1−3] arc discharge,[4] or the heating of C_{60} encapsulated in SWCNTs.[5] However, catalytic particles, amorphous carbon, or damaged tubes in the as-produced samples may impair potential applications. Furthermore, the final product usually contains tubes with a wide diameter distribution varying between several synthesis methods. Although removal of some catalyst particles occurs by acid treatments, oxidation in air or oxidizing acids has been found to selectively remove amorphous carbon and unwanted tubes,[6−10] but weight losses can exceed 90% after purification. Accurate control of the purification processes is needed for determining ideal oxidation conditions that lead to the removal of impurities without loss or damage of valuable nanotubes. In situ Raman spectroscopy observes the kinetics of oxidation and provides time-resolved information about structural changes while the tubes are treated. Other investigation methods, such as high-resolution transmission electron microscopy (HRTEM) and thermogravimetric analysis (TGA), may be needed to complement the Raman data.

Raman spectroscopy has become a popular tool for the characterization of the structure and properties of carbon allotropes.[11,12] In a typical Raman spectrum of SWCNTs, three features identified as the radial breathing modes (RBM)

* To whom correspondence should be addressed. Fax: 215-895-1934. E-mail: gogotsi@drexel.edu.
† Drexel University.
‡ Université Paul Sabatier.

(1) Flahaut, E.; Peigney, A.; Laurent, C.; Rousset, A. *J. Mater. Chem.* **2000**, *10*, 249−252.
(2) Ci, L. J.; Rao, Z. L.; Zhou, Z. P.; Tang, D. S.; Yan, Y. Q.; Liang, Y. X.; Liu, D. F.; Yuan, H. J.; Zhou, W. Y.; Wang, G.; Liu, W.; Xie, S. S. *Chem. Phys. Lett.* **2002**, *359* (1−2), 63−67.
(3) Flahaut, E.; Bacsa, R.; Peigney, A.; Laurent, C. *Chem. Commun.* **2003**, *12* (12), 1442−1443.
(4) Hutchison, J. L.; Kiselev, N. A.; Krinichnaya, E. P.; Krestinin, A. V.; Loutfy, R. O.; Morawsky, A. P.; Muradyan, V. E.; Obraztsova, E. D.; Sloan, J.; Terekhov, S. V.; Zakharov, D. N. *Carbon* **2001**, *39* (5), 761−770.
(5) Bandow, S.; Hiraoka, T.; Yumura, T.; Hirahara, K.; Shinohara, H.; Iijima, S. *Chem. Phys. Lett.* **2004**, *384* (4−6), 320−325.
(6) Bandow, S.; Takizawa, M.; Hirahara, K.; Yudasaka, M.; Iijima, S. *Chem. Phys. Lett.* **2001**, *337* (1−3), 48−54.
(7) Borowiak-Palen, E.; Pichler, T.; Liu, X.; Knupfer, M.; Graff, A.; Jost, O.; Pompe, W.; Kalenczuk, R. J.; Fink, J. *Chem. Phys. Lett.* **2002**, *363* (5−6), 567−572.
(8) Flahaut, E.; Peigney, A.; Laurent, C.; Rousset, A. *J. Mater. Chem.* **2000**, *10* (2), 249−252.
(9) Gajewski, S.; Maneck, H. E.; Knoll, U.; Neubert, D.; Dorfel, I.; Mach, R.; Strauss, B.; Friedrich, J. F. *Diamond Relat. Mater.* **2003**, *12* (3−7), 816−820.
(10) Li, W. Z.; Wen, J. G.; Sennett, M.; Ren, Z. F. *Chem. Phys. Lett.* **2003**, *368* (3−4), 299−306.
(11) Thomsen, C.; Reich, S.; Maultzsch, J. *Philos. Trans. R. Soc. London, Ser. A* **2004**, *362* (1824), 2337−2359.
(12) Ferrari, A. C.; Robertson, J. *Philos. Trans. R. Soc. London, Ser. A* **2004**, *362* (1824), 2477−2512.

10.1021/cm052755g CCC: $33.50
Published on Web 02/22/2006

(below 400 cm^{-1}), D-band (1300−1350 cm^{-1}), and G-band (tangential mode, 1590 cm^{-1}) are present. Whereas the frequency of the RBM is inversely proportional to the tube diameter and is often used for its determination,[13] the D-band of the CNTs is a double resonance band mainly originating from defects in tube walls and disordered material surrounding the tubes.[11] It should be noted that different types of tubes contribute to the D band intensity in different ways. They show different absorption and light-scattering behavior depending on their chirality and thus on their electronic properties.[11] The intensity and position of the D band depends on defect distributions, tube diameter, and the presence of nontubular carbon.[14]

The Raman spectrum of the DWCNTs has been found to be very similar and comparable to that of SWCNTs because of their small diameters.[6,15] Their interlayer distance varies around 0.3−0.4 nm according to theoretical calculations,[16] and the Raman modes of both inner and outer tubes can be observed.

The G band of single- and double-walled tubes is a more complex Raman feature compared to the G band of single-crystal graphite. Raman-active modes between 1500 and 1600 cm^{-1} result from C═C bond stretching motions in carbon nanotubes.[17,18] Because of symmetry-breaking effects associated with the tube curvature and thus the folding of the graphite Brillouin zone into the Brillouin zone of a nanotube, the G band of graphite splits into several modes that show different symmetries.[19] For a SWCNT sample, six Raman-active modes are predicted and usually observed in this particular frequency range.[20,21] The three upper frequencies are associated with vibrations along the tube axis and named G^+. Vibrations along the circumference of the tube leading to an additional three frequencies are labeled G^-.[17] The G^- band is broader for metallic tubes compared to the narrow Lorentzian peak of semiconducting nanotubes. The splitting between G band components can also be used for diameter analysis.[17] For DWCNTs, in which the G band can be found from an overlap of tangential vibrations from both inner and outer tubes, similar splitting is observed. The mode splitting decreases with increasing outer-tube diameter.[22] Thus, we expect a broader band for DWCNTs compared to the G band of SWCNTs because the DWCNT samples contain a broader size distribution with respect to larger outer and smaller inner tubes.

In situ Raman monitoring of temperature treatments of nanotubes and other forms of carbon has been reported in the literature and helped us to determine the oxidation conditions for DWCNTs and amorphous carbon.[23] Temperature-induced shifts of the first-order Raman peaks have been reported by several groups.[24−26] It is also well-known that peak positions and Raman intensities of RBM and G bands show resonant effects dependent on the excitation wavelength.[17,27] RBM are often strong enough to appear observable only in the Raman spectra when the incident laser energy coincides with the energy range of real electronic excitation or transition (resonant Raman effect).

In this paper, we present a detailed report on the in situ Raman spectroscopy study of the oxidation of DWCNTs and compare it with the oxidation of SWCNTs upon isothermal and nonisothermal heating in air. The focus of this investigation was on the removal of disordered carbon and understanding the associated changes in the Raman spectra that occur during heating and oxidation.

Experimental Section

Materials. DWCNTs were produced by a CCVD method using a $Mg_{1-x}Co_xO$ solid solution catalyst containing Mo oxide.[3] The use of Mo in addition to Co or Fe has been reported to increase the DWCNT yield in the CCVD synthesis and the selectivity of forming other tubes. The obtained raw CCVD samples were treated with a concentrated HCl solution to dissolve the catalyst. The suspension of CNTs was then washed with deionized water until neutrality and subsequently filtered. Finally, the sample was dried overnight at 80 °C in air. The detailed experimental description of the synthesis procedure for the studied DWCNTs was published elsewhere.[3]

SWCNT samples came from Tubes@Rice and were prepared by the HiPCO process.[28] SWCNTs were grown on catalytic clusters of iron at pressures between 30 and 50 atm, and temperatures around 900−1100 °C from flowing CO. The raw material was purified to eliminate the Fe catalyst and amorphous carbon as described by Bronikowski et al.[28]

Methods. The samples were heated in a LINKAM THM600 heating stage in static laboratory air at ambient pressure. The nanotube powder was dispersed in ethanol to produce a thin film of carbon nanotubes on a glass slide. The slide was placed on a silver holder inside the hot stage. The tubes were kept in the stage and placed under the microscope. The stage was calibrated by using the melting points of $AgNO_3$ (209 °C), tin (232 °C), KNO_3 (334

(13) Bandow, S.; Asaka, S.; Saito, Y.; Rao, A. M.; Grigorian, L.; Richter, E.; Eklund, P. C. *Phys. Rev. Lett.* **1998**, *80* (17), 3779−3782.
(14) Dillon, A. C.; Yudasaka, M.; Dresselhaus, M. S. *J. Nanosci. Nanotechnol.* **2004**, *4* (7), 691−703.
(15) Ren, W.; Li, F.; Chen, J.; Bai, S.; Cheng, H.-M. *Chem. Phys. Lett.* **2002**, *359* (3−4), 196.
(16) Charlier, A.; McRae, E.; Heyd, R.; Charlier, M. F.; Moretti, D. *Carbon* **1999**, *37*, (11), 1779.
(17) Jorio, A.; Souza, A. G.; Dresselhaus, G.; Dresselhaus, M. S.; Swan, A. K.; Unlu, M. S.; Goldberg, B. B.; Pimenta, M. A.; Hafner, J. H.; Lieber, C. M.; Saito, R. *Phys. Rev. B* **2002**, *65* (15).
(18) Kasuya, A.; Sasaki, Y.; Saito, Y.; Tohji, K.; Nishina, Y. *Phys. Rev. Lett.* **1997**, *78* (23), 4434−4437.
(19) Pimenta, M. A.; Marucci, A.; Brown, S. D. M.; Matthews, M. J.; Rao, A. M.; Eklund, P. C.; Smalley, R. E.; Dresselhaus, G.; Dresselhaus, M. S. *J. Mater. Res.* **1998**, *13* (9), 2396−2404.
(20) Balkanski, M. *Physical Properties of Carbon Nanotubes*; Saito, R., Dresselhaus, G., Dresselhaus, M. S., Eds.; Imperial College Press: London, 1998; *Mater. Sci. Eng., B* **2000**, *76* (3), 241.
(21) Jorio, A.; Dresselhaus, G.; Dresselhaus, M. S.; Souza, M.; Dantas, M. S. S.; Pimenta, M. A.; Rao, A. M.; Saito, R.; Liu, C.; Cheng, H. M. *Phys. Rev. Lett.* **2000**, *85* (12), 2617−2620.
(22) Rahmani, A.; Sauvajol, J. L.; Cambedouzou, J.; Benoit, C. *Phys. Rev. B* **2005**, *71* (12).
(23) Osswald, S.; Flahaut, E.; Ye, H.; Gogotsi, Y. *Chem. Phys. Lett.* **2005**, *402* (4−6), 422−427.
(24) Ci, L. J.; Zhou, Z. P.; Song, L.; Yan, X. Q.; Liu, D. F.; Yuan, H. J.; Gao, Y.; Wang, J. X.; Liu, L. F.; Zhou, W. Y.; Wang, G.; Xie, S. S. *Appl. Phys. Lett.* **2003**, *82* (18), 3098−3100.
(25) Rao, A. M.; Richter, E.; Bandow, S.; Chase, B.; Eklund, P. C.; Williams, K. A.; Fang, S.; Subbaswamy, K. R.; Menon, M.; Thess, A.; Smalley, R. E.; Dresselhaus, G.; Dresselhaus, M. S. *Science* **1997**, *275* (5297), 187−191.
(26) Raravikar, N. R.; Keblinski, P.; Rao, A. M.; Dresselhaus, M. S.; Schadler, L. S.; Ajayan, P. M. *Phys. Rev. B* **2002**, *66* (23).
(27) Jorio, A.; Saito, R.; Hafner, J. H.; Lieber, C. M.; Hunter, M.; McClure, T.; Dresselhaus, G.; Dresselhaus, M. S. *Phys. Rev. Lett.* **2001**, *86* (6), 1118−1121.
(28) Bronikowski, M. J.; Willis, P. A.; Colbert, D. T.; Smith, K. A.; Smalley, R. E. *J. Vac. Sci. Technol., A* **2001**, *19* (4), 1800−1805.

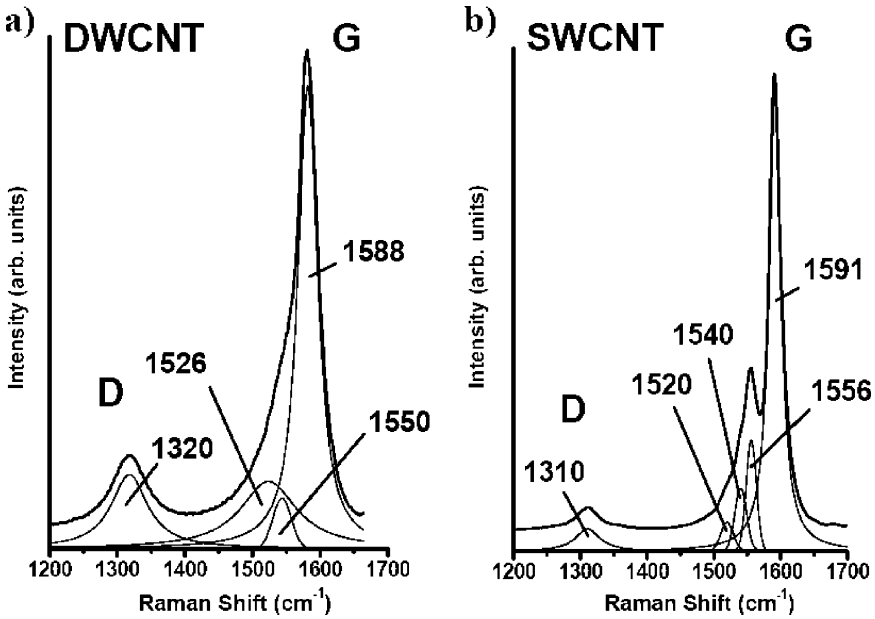

Figure 1. Comparison of room-temperature Raman spectra of as-received (a) DWCNT and (b) SWCNT showing differences in the D/G ratio and the peak splitting within the G band. Spectra were recorded using a 633 nm excitation wavelength.

°C), and $Ca(OH)_2$ (580 °C). In every case, the difference between the measured and expected melting point did not exceed 2 °C (for 5 °C/min heating).

The oxidation process followed two different heating procedures. The first procedure (nonisothermal) includes heating from room temperature to 600 °C with a rate of 5 °C/min while holding at each measurement temperature for about 4 min. Spectra were taken in steps of 50 °C in the range 50−350 °C, followed by 25 °C steps from 350 to 400 °C and 10 °C steps from 400 to 600 °C. After reaching the desired temperature, the sample was cooled at 20 °C/min until it reached 80 °C and then cooled at 10 °C/min down to room temperature. This is comparable to a continuous heating rate of 3 °C/min without steps. In the second oxidation procedure (isothermal), samples were heated at 50 °C/min and exposed to the desired temperature for 330 min. In that case, Raman spectra were acquired every 15 min after reaching the dwell temperature. After 330 min, the sample was cooled at a 50 °C/min rate until it reached 80 °C followed by cooling at ∼10 °C/min to room temperature. Isothermal oxidation experiments were carried out at 350, 365, 370, 375, 400, 430, 440, 475, and 550 °C. In the case of isothermal oxidations, the heating rate was 50 °C/min under the same atmospheric conditions that were used for nonisothermal oxidations.

Raman spectra were recorded with a Renishaw 1000 spectrometer using an Ar^+ ion laser (514.5 nm, 2.14 eV), a HeNe laser (633 nm, 1.96 eV) and a diode laser (780 nm, 1.59 eV) in backscattering geometry. Long focus objectives (20× and 50×) were used to protect the equipment against the heat produced by the stage. The laser beam was slightly defocused to guarantee a larger measurement area for better statistical results and a lower laser power density to avoid laser-induced sample heating. To minimize the influence of sample inhomogeneities, every measurement was done at the same spot during an oxidation experiment. This appeared difficult with respect to heating-induced sample drift. All measurements were repeated five times to produce statistically reliable results. The Raman peak positions, at various temperatures, were determined by a peak-fitting procedure using the standard GRAMS-32 software and a mixed Gaussian−Lorentzian function for the peak shape. Integral intensities of Raman bands were used in calculating the R ratio.

Thermogravimetric analysis (TGA) was carried out using a SETARAM TAG24 operated in static air. In the TGA experiments, the sample was heated from 25 to 600 °C at 5 °C/min with no steps until 400 °C. This heating rate was constant during the whole measurement. To simulate the conditions of the in situ Raman experiment, 4 min isothermal steps were done at 400, 420, 430, and 440 °C. Additional 8 min steps followed at 460 and 500 °C. Slight differences between TGA and Raman spectroscopy results may be induced by the impossibility of reproducing the exact experimental conditions of the in situ Raman measurements in the TGA. Sample size and the conditions within the stage may also have some non-negligible influence. A potential problem in the hot stage experiments might be insufficient air circulation and oxidation in the oxygen-lean $O_2-CO-CO_2$ atmosphere. However, experiments with the opened stage showed no significant changes in the results, so the influence of the small volume appears to be negligible.

Results and Discussion

Raman Spectra of the As-received Nanotubes. Figure 1 compares the D and G bands of DWCNTs (a) and SWCNTs (b), recorded using a 633 nm laser excitation. The G band of the as-received DWCNTs can be fitted with Lorentzian peaks at 1588 cm^{-1} (G^+) and 1550 cm^{-1} (G^-) and a broad Gaussian peak around 1526 cm^{-1}. Whereas narrow Lorentzian peaks are ascribed to semiconducting nanotubes, the broader peaks are attributed to metallic tubes[29,30] or may also result from an overlap of peaks coming from tubes with different diameters. DWCNTs show a larger $R = I_D/I_G$ ratio (∼0.25) compared to that of SWCNTs (∼0.07). Whereas the Raman spectra acquired with a 514 nm laser wavelength give an R of approximately 0.22, this value increases to 0.40 for the 780 nm laser excitation because of different Raman scattering cross sections of the D band Raman mode for each laser wavelength. Furthermore, the D band position shows the dependence on the excitation

(29) Kataura, H.; Kumazawa, Y.; Maniwa, Y.; Umezu, I.; Suzuki, S.; Ohtsuka, Y.; Achiba, Y. *Synth. Met.* **1999**, *103* (1−3), 2555−2558.
(30) Brown, S. D. M.; Jorio, A.; Corio, P.; Dresselhaus, M. S.; Dresselhaus, G.; Saito, R.; Kneipp, K. *Phys. Rev. B* **2001**, *6315* (15).

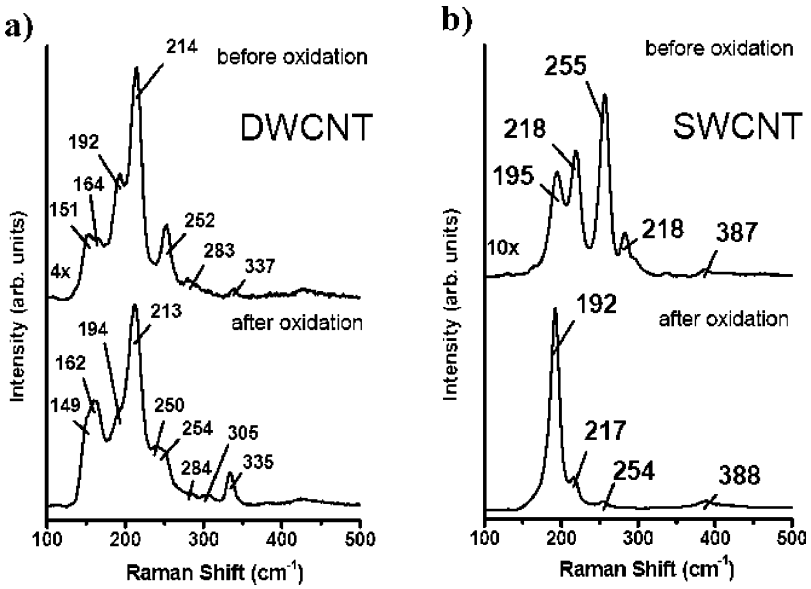

Figure 2. RBM frequency range of the Raman spectra of (a) DWCNTs and (b) SWCNTs before and after nonisothermal oxidation. The RBMs of the DWCNTs show no significant changes after oxidation, suggesting that oxidation of the nanotubes did not occur. The RBMs of the SWCNT sample show structural changes within the sample, starting with the oxidation of smaller tubes and the disappearance of higher RBM frequencies. Spectra were acquired at room temperature using a 633 nm laser excitation.

wavelength too, which is a characteristic feature of a double-resonance process.[11]

In the case of SWCNTs, there is a larger G band splitting with respect to the G^- and G^+ Raman modes, and three different peaks (1556, 154,0 and 1520 cm^{-1}) resulting from the transversal radial vibrations contributing to G^- can be observed. A lower *R* value for the SWCNT sample suggests a smaller concentration of structural defects and/or amorphous material.

The as-received DWCNTs show several Raman features between 130 and 340 cm^{-1} (Figure 2a). These peaks originate in collective radial vibrations of all carbon atoms and are strongly influenced by the resonant Raman effect.[25] Similarly for SWCNTs, these frequencies are inversely proportional to the tube diameters. The diameter dependence of the RBM frequencies of a DWCNT is given by the equation: $\omega = \alpha/d$, where ω (cm^{-1}) is the RBM frequency, *d* (nm) is the diameter of the tube, and α is a constant. van der Waals interactions between the outer and inner tubes may lead to some mixed vibrational modes in the RBM range. However, we assume that this interaction does not significantly affect the basic vibrations of the outer and inner tubes compared with those of their SWCNT counterparts.[25] Values of α between 223 and 236 cm^{-1} have been reported in the literature.[25,31−33] Neglecting tube−tube interactions, we used an average value of α=224 cm^{-1} to calculate the tube diameters. Combining theoretical calculations and experimental results, we have to consider tube−tube interactions within bundles and also the interactions between the outer and inner tubes. If we simply suppose that the influence of van der Waals interactions in DWCNTs is similar to the behavior of SWCNTs within bundles, we can define $\omega = 238/d^{0.93}$.[34−36]

Table 1. Nanotube Diameters Calculated from the RBM of DWCNT Using 514.5, 633, and 780 nm Laser Excitation

inner tubes		outer tubes	
d (nm)	f_{RBM} (cm^{-1})	*d* (nm)	f_{RBM} (cm^{-1})
1.18	204	1.90	131
1.12	213	1.65	149
1.07	223	1.51	162
1.03	231	1.35	180
0.96	247	1.28	189
0.93	254	1.24	194
0.90	263		
0.83	284		
0.81	290		
0.77	305		
0.69	335		

The smallest observed inner diameter for DWCNTs is 0.40 nm, with an interlayer spacing of 0.34 nm between the outer tube and the inner tube, and leads to the conclusion that all RBM frequencies higher than 200 cm^{-1} must be ascribed to inner tubes, whereas lower frequencies can be associated with both inner and outer tubes. Peaks between 130 and 340 cm^{-1} correspond to a diameter range of 0.7−1.9 nm (Table 1), which is within the range of diameters (0.53−2.53 nm for inner and 1.2−3.23 nm for outer tubes) determined from HRTEM.[3] The resonance enhancement for laser energies between 1.59 and 2.41 eV mostly favors the vibration modes above 200 cm^{-1}.[37] It is important to note that the intensities do not reflect the real amount of individual tubes because

(31) Kurti, J.; Kresse, G.; Kuzmany, H. *Phys. Rev. B* **1998**, *58* (14), R8869−R8872.
(32) Rahmani, A.; Sauvajol, J. L.; Rols, S.; Benoit, C. *Phys. Rev. B* **2002**, *66* (12).
(33) Sanchez-Portal, D.; Artacho, E.; Soler, J. M.; Rubio, A.; Ordejon, P. *Phy. Rev. B* **1999**, *59* (19), 12678−12688.
(34) Rao, A. M.; Chen, J.; Richter, E.; Schlecht, U.; Eklund, P. C.; Haddon, R. C.; Venkateswaran, U. D.; Kwon, Y. K.; Tomanek, D. *Phys. Rev. Lett.* **2001**, *86* (17), 3895−3898.
(35) Alvarez, L.; Righi, A.; Rols, S.; Anglaret, E.; Sauvajol, J. L. *Chem. Phys. Lett.* **2000**, *320* (5−6), 441−447.
(36) Henrard, L.; Hernandez, E.; Bernier, P.; Rubio, A. *Phys. Rev. B* **1999**, *60* (12), R8521−R8524.
(37) Ci, L. J.; Zhou, Z. P.; Yan, X. Q.; Liu, D. F.; Yuan, H. J.; Song, L.; Gao, Y.; Wang, J. X.; Liu, L. F.; Zhou, W. Y.; Wang, G.; Xie, S. S.; Tan, P. H. *J. Appl. Phys.* **2003**, *94* (9), 5715−5719.

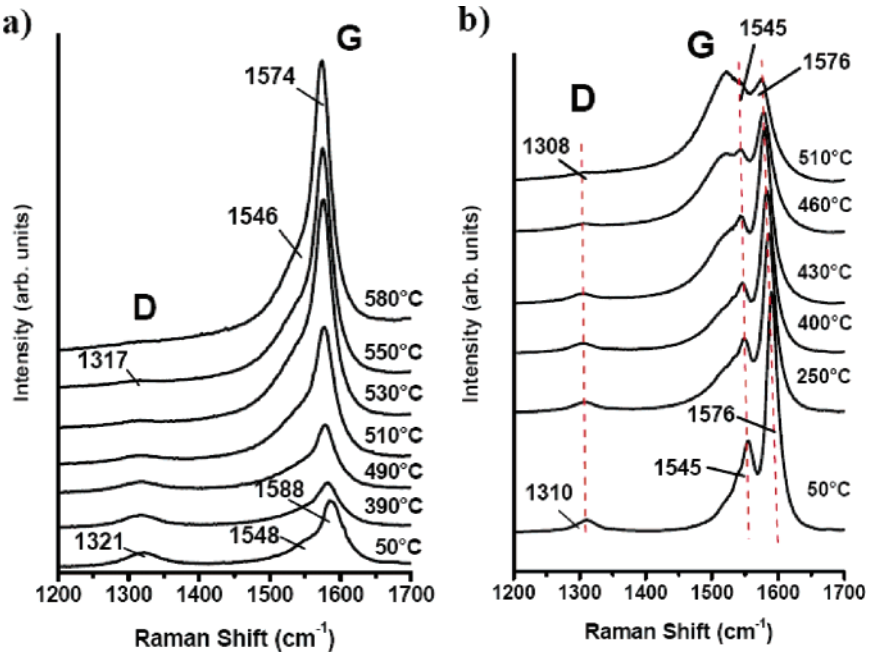

Figure 3. (a) Nonisothermal oxidation of DWCNT leads to a significant increase in the G band intensity upon heating induced by the oxidation of amorphous carbon, whereas the D band disappears. (b) The increase in G band intensity was not observed during the nonisothermal oxidation of SWCNT, which is explained by the existence of only a small amount of amorphous material in that sample, which was already purified. Spectra were recorded using a 633 nm excitation wavelength.

of the resonance effect, which amplifies the Raman signal from certain tubes. The RBM spectra of SWCNTs (Figure 2b) show a narrower diameter distribution compared to that of DWCNTs, as expected. For the investigated SWCNTs, the RBM peaks are between 190 and 220 cm^{-1}. Furthermore, the RBM spectra of the SWCNT samples exhibit a lower number of peaks but with a higher relative intensity compared to the RBM intensity of DWCNTs. This can also be explained by the smaller diameter distribution within the SWCNT sample and the fact that the RBM spectra of DWCNTs are an overlap of the Raman signals coming from both inner and outer tubes. Thus the RBM spectra of DWCNTs have a wider frequency range, but with a lower intensity.

In situ Raman Study. *Non-Isothermal Oxidation.* Figure 3a shows the Raman spectra of DWCNTs during the heat treatment acquired with the 633 nm laser excitation. The *R* ratio starts to decrease above 450 °C until the D band, which is attributed to amorphous carbon and structural defects, nearly disappears upon reaching 550 °C. Please note that the Raman spectra in Figure 3 show only the *R* ratio change, not the absolute values for D or G band intensities, as both bands may change in intensity at elevated temperatures, which leads to a change in *R*.[23] The temperature range in which changes occur may change slightly, depending on the amount of material and heat-transfer conditions at the measured spot. The D band intensity increases with the excitation wavelength.

Figure 3b shows Raman spectra during the oxidation of a SWCNT sample. No significant changes in the *R* ratio are observed below 400 °C. Up to 500 °C, a decrease in the D band intensity and the *R* ratio together with a decrease in the G band intensity serves as a clear sign for the oxidation of disordered carbon and nanotubes.

As expected, we found a linear downshift in the D and G band of SWCNTs and DWCNTs with temperature; DWCNTs exhibit different frequency shifts of peaks, giving rise to the G band Raman signal. Thermal shifts of 0.024 cm^{-1}/°C have been reported for high purity natural graphite (1580 cm^{-1}) and 0.03 cm^{-1}/°C for SWCNTs.[25] Our experiments with DWCNTs (Figure 4a) using a 633 nm wavelength excitation show a downshift of 0.029 cm^{-1}/°C for 1568 and 1525 cm^{-1} peaks, which were fitted as one peak at 1550 cm^{-1}, and a value of 0.026 cm^{-1}/°C for the peak at 1588 cm^{-1}. Oxidation of SWCNTs (Figure 4b) yields downshifts of 0.030 cm^{-1}/°C for the G^- peak around 1558 cm^{-1} and 0.028 cm^{-1}/°C for the peak at 1591 cm^{-1} (G^+). Thus the value of temperature-induced shifts of the G band frequencies in the DWCNTs Raman spectra is between the values of those for SWCNTs and graphite.[24]

The temperature dependencies of the D band vary slightly for SWCNTs and DWCNTs and have been found experimentally to be ~0.013 and 0.015 cm^{-1}/°C, respectively, in agreement with published data.[38] The phenomenon of different G mode shifts within the spectra of DWCNTs has also been observed.[24] The order of magnitude of the downshift depends on the laser-power density with regard to laser-induced heating.

The *R* ratio of DWCNTs in a certain temperature range does not directly represent the degree of disorder or purity within our DWCNT sample with respect to the absolute D band intensity. Previous experiments [23] show an increase in the G band intensity occurring about 20−30 °C before a significant decrease in the D band, resulting in the initial decrease in *R*. It has been found that the intensity of the G band starts to increase at ~440 °C and reaches a maximum

(38) Huang, F. M.; Yue, K. T.; Tan, P. H.; Zhang, S. L.; Shi, Z. J.; Zhou, X. H.; Gu, Z. N. *J. Appl. Phys.* **1998**, *84* (7), 4022−4024.

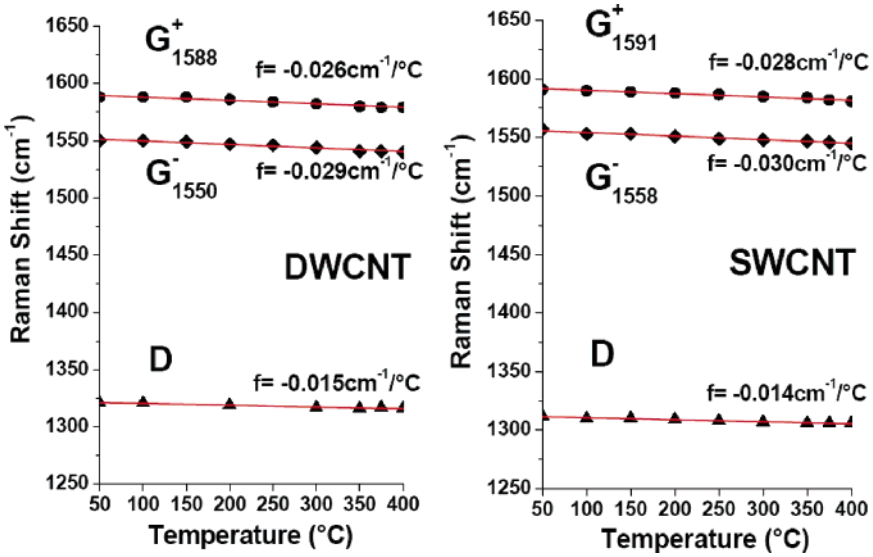

Figure 4. Comparison of temperature-induced frequency shifts of the D, G^+, and G^- bands of (a) DWCNTs and (b) SWCNTs, recorded using a 633 nm laser excitation.

near 500 °C.[23] The origin of the observed behavior of the D and G bands can be explained by the removal of adsorbed species or disordered carbon on the tube surface, which may shield the Raman signal from the tubes. Analysis of similar experiments done with a previously oxidized DWCNT sample using in situ Raman spectroscopy showed no significant changes in the G band intensity during treatment. This clearly demonstrates that an increase in the G band intensity followed by a decreasing *R* ratio cannot be due to temperature effects and must be ascribed to the removal of surface species. Thus, we conclude that the purified SWCNT sample showing no increase in the G band intensity contains less amorphous carbon, which may shield the tubes, than DWCNTs. Because SWCNTs were purified after synthesis, we attribute the D band mostly to defects within the tubes. This is supported by the fact that the D and G bands behave in a similar manner at temperatures above 400 °C. These structural changes are also supported by changes in the RBM range of the Raman spectra (Figure 2b). Small diameter tubes, showing higher RBM frequencies compared to larger tubes, start to decrease in intensity or even disappear after the oxidation, which is in agreement with previous studies.[39] The higher-intensity Raman spectra from the oxidized samples compared to the as-received tubes can be explained by the oxidation of amorphous carbon and damaged tubes. The peak splitting within the G band becomes more pronounced after heat treatment.[23] The observed irreversible shifts, which do not disappear during cooling to room temperature, are due to changes in the contributions of different G band components rather than to temperature-induced shifts. This change can occur because of the selective oxidation of several carbon species contributing to the G band. As the Raman signal of amorphous carbon or small-diameter nanotubes disappears, the position, intensity, and shape of the G band, resulting from an overlap of different vibrational modes, changes. It has been reported that the frequency of the Raman mode around 1590 cm^{-1} (G^+) shows little to no diameter dependence.[17] Thus, no changes are expected during heating even in the case of the oxidation of several carbon species within the sample. The presented in situ experiments of DWCNTs and SWCNTs support this assumption, especially because the G^+ mode frequencies are almost the same before and after heating. Although the peaks at 1588 and 1576 cm^{-1} for DWCNTs and SWCNTs, respectively, show no frequency shift in the G band due to compositional changes, the lower frequency G^- band clearly depends on the diameter distribution and sample purity.

The most impressive observation so far was a complete oxidation of disordered carbon leading to the disappearance of the D band in the DWCNT sample. The Raman spectra acquired using 514.5 nm laser excitation did not show the D band after oxidation (Figure 3a). Even for the 780 nm laser wavelength (not shown), which enhances the D band intensity, the *R* ratio decreased from its original value of 0.43 to ~0.015 after oxidation.[23]

Selective Oxidation of Small-Diameter Tubes. An increase in the Raman intensity is generally observed at about 400 °C, the temperature range in which the disordered carbon is oxidized and the G band intensity increases. The subsequent decrease in intensity at higher temperature is due to the oxidation of tubes, starting with the smallest tubes within the sample. Even after oxidation at temperatures above 500 °C, the RBMs do not always show significant changes. We assume that changes in the structure and composition of the sample above 500 °C strongly depend on the duration of oxidation as well as the temperature. The oxidation was never completed and usually stopped at different temperatures between 550 and 600 °C when the Raman signal of carbon was still recordable. We also observed new peaks appearing at temperatures higher than 500 °C at 475, 520, and 683 cm^{-1} that can be attributed to the cobalt oxide, which is formed by the oxidation of trace catalytic particles remaining in the sample, and should be ignored.[23]

Figure 5 shows the in situ Raman analysis of the low-frequency RBM range for DWCNTs, acquired using three

(39) Zhou, W.; Ooi, Y. H.; Russo, R.; Papanek, P.; Luzzi, D. E.; Fischer, J. E.; Bronikowski, M. J.; Willis, P. A.; Smalley, R. E. *Chem. Phys. Lett.* **2001**, *350* (1−2), 6−14.

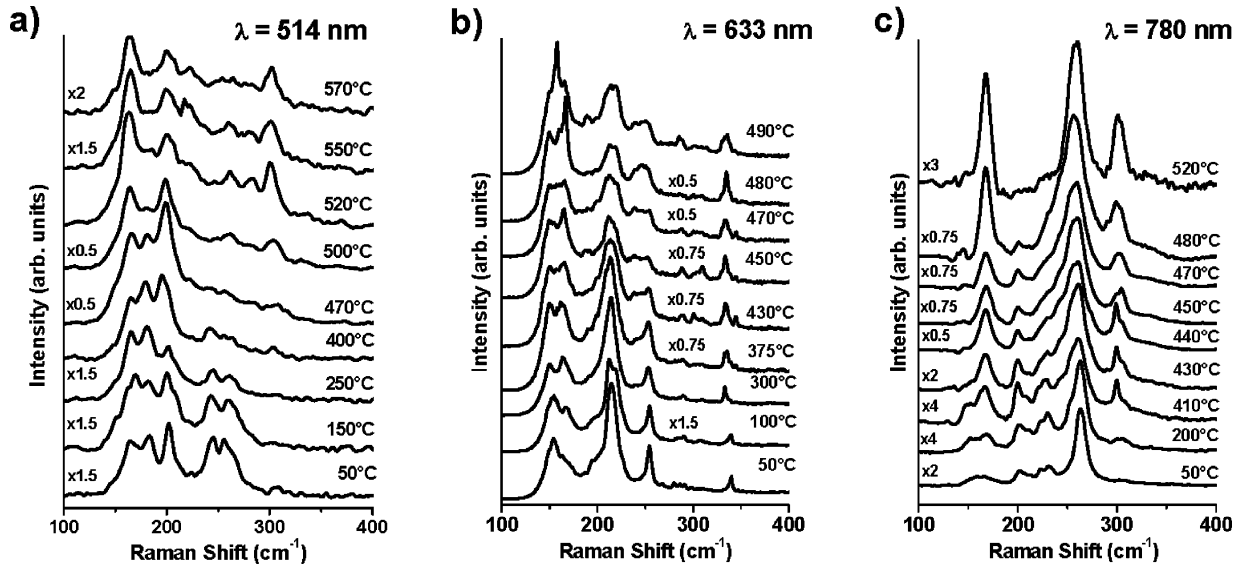

Figure 5. Multiwavelength Raman spectra of DWCNTs recorded in situ using a (a) 514.5, (b) 633, and (c) 780 nm laser excitation. The spectra show temperature-induced changes even before the oxidation of any carbon material starts (<400 °C). The different laser wavelengths show different changes due to different resonance enhancement. At higher temperatures (>400 °C), the intensity of several Raman peaks in the higher RBM frequency range (300−350 cm^{-1}) increases because of the oxidation of outer tubes and the increasing detection of Raman scattering of the inner tubes.

different laser excitation wavelengths. The intensity of the peaks between 220 and 280 cm^{-1} decreases constantly during heating from room temperature to 400 °C (Figure 5a). As there are no observable changes in the D and G band shape or intensity, these changes cannot be attributed to structural changes because of the selective oxidation of some tubes.

It is important to mention that there is a temperature-induced downshift of RBM peaks, which is less pronounced than shifts in the G or D bands, although it is still observable. It shows a linear behavior as well. The shift is larger for lower frequencies originating in the larger diameter tubes and smaller for higher RBM frequencies.[24] In situ measurements under heating of DWCNTs at 5 °C/min up to 400 °C directly followed by cooling to room temperature show certain RBM peaks decreasing and increasing in intensity while the sample is heated or cooled, respectively. These changes are due to temperature effects and are completely reversible. These temperature effects are somewhat different for frequencies originating from tubes of different diameters due to the resonance effect that occurs when using different excitation wavelengths, but are nevertheless observable in each experiment. A shift due to the resonance enhancement can be caused not only by changing the laser wavelength but also by changing the temperature, leading to decreasing and increasing intensities during heating or cooling, respectively. However, because the comparison of the RBM spectra of DWCNTs before and after heating shows no significant changes (Figure 1c), we assign the effect of the varying RBM intensity upon heating (Figure 5) to the temperature effect on the C═C bonding. Although the influence of the oxidation of the tubes on the RBM intensity seems to be negligible below 500 °C, the oxidation increases and dominates the in situ Raman spectra at higher temperatures (550−600 °C).

The in situ RBM Raman spectra of the DWCNTs show the highest intensities in the temperature range between 450 and 500 °C. In this temperature range, the G band reaches a maximum intensity, whereas the D band disappears. The small amount of amorphous carbon within the as-received DWCNT sample shields RBM Raman scattering similar to the G band Raman signal, and thus oxidation improves the intensity of the Raman signal of the DWCNTs in general. After reaching a maximum intensity around 500 °C, the RBMs then decrease because of the oxidation of several tubes. The intensity of the RBMs and the G band exhibit similar behavior with respect to the removal of amorphous carbon. Furthermore, it can be seen that after reaching high temperatures above 400 °C, the intensity of several peaks in the higher-frequency region of the RBM range between 300 and 350 cm^{-1} starts to increase. This can be explained by the oxidation of certain outer tubes and the increase in the detection of the Raman scattering of the smaller inner tubes that exhibit higher RBM frequencies. The inner tubes are not oxidized before the outer ones are damaged or destroyed. The oxygen molecules cannot go through the outer walls and thus are not able to reach the carbon atoms inside the closed tubes.

Isothermal Oxidation. In nonisothermal oxidation experiments, the G band does not decrease at temperatures below 480 °C, suggesting that oxidation does not occur in the tubes but does for the amorphous carbon below this temperature. However, these experiments did not provide information about the kinetics of the process or the minimal temperature requirement for the removal of amorphous carbon. To understand the kinetics of oxidation, a treatment under isothermal conditions was used. Figure 6a shows the *R* ratio change as a function of time. Below 365 °C, no changes are observed. Neither amorphous carbon nor other carbon species appear to oxidize under these conditions. This is in agreement with Figure 6b, which shows no D band area change below 365 °C. The same behavior can be observed while looking at the G band area. The activation energy needed for breaking the carbon bonds is not provided below that temperature. The first changes in the *R* ratio are observed at 370 °C (Figure 6a). In these experiments, the ratio decreased from

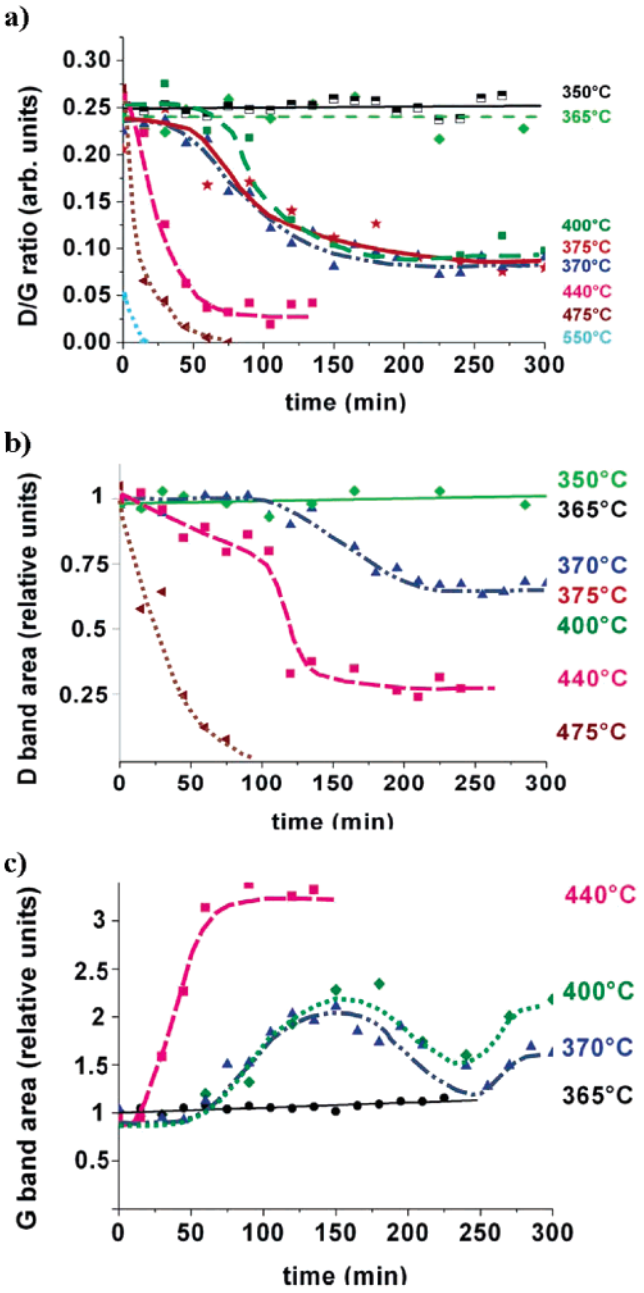

Figure 6. Results of isothermal oxidation of the DWCNTs showing the (a) *R* ratio (D/G), (b) relative D band intensity, and (c) relative G band intensity as a function of the oxidation time at different temperatures. Spectra were recorded using a 633 nm excitation wavelength. The curves for 350 and 365 °C in panel b are superimposed, and idem for 370, 375, and 400 °C.

∼0.25 to approximately 0.08. The ratio starts to decrease after the 20−50 min incubation period, which may be required for oxygen chemisorption or the removal of functional groups from the carbon surface, reaches the final value of 0.08 after 220−240 min, and does not show further changes with time. In the range of 370−400 °C, similar changes in the *R* value are observable, suggesting that only the amorphous carbon is oxidized and the tubes are not effected by oxidation. The incubation period disappears and the *R* value decreases further to zero after a relatively short time as the processing temperature increases from 440 to 550 °C. We believe that defective and small-diameter tubes are oxidized in this temperature range, leading to the

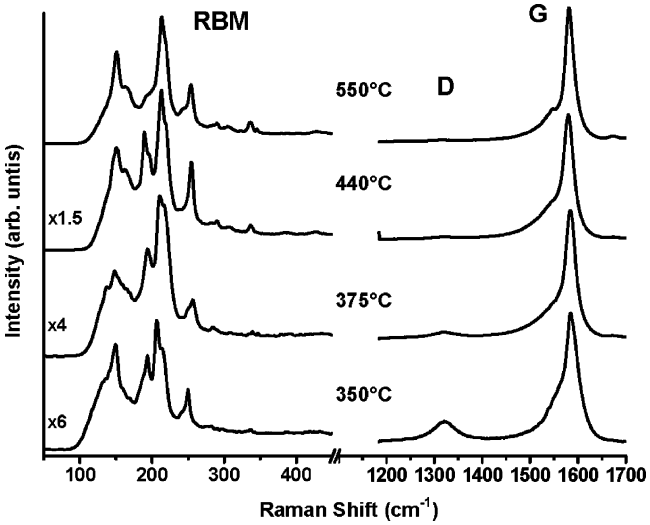

Figure 7. First-order Raman spectra of DWCNT after isothermal oxidation at different temperatures recorded at room temperature using a 633 nm laser excitation. The *R* value shows no changes for oxidation temperatures below 350 °C. At higher temperatures, *R* reaches a minimum after a certain time, depending on the temperature, until it becomes zero at 550 °C (D band disappears).

disappearance of the D band. To determine the exact reason for the decrease in the *R* ratio, we must investigate the D and G bands separately. In the case of 370, 375, and 400 °C, the D band area shows behavior similar to *R*. The relative value of the D band decreases to about 35% of its original value, whereas the *R* ratio decreases by ∼65%. An explanation for the difference can be seen in Figure 6c. The decrease in the D band intensity is closely related to a large increase in the G band area. Between the 50th and 150th minute, a small decrease in the D band area (10−15%) is accompanied by a doubling of the G band area, ending in a large decrease in *R*. After about 150 min, the G band area and *R* reach a maximum and minimum, respectively. The subsequent decrease in the D band does change the *R* ratio significantly, because the G band area and intensity are decreasing as well. The isothermal oxidations at 440, 470, and 550 °C show different behavior, as shown in Figure 6a. The *R* ratio starts to decrease upon heating because oxidation of the amorphous carbon starts before reaching the final temperature. Although 440 °C is not high enough to eliminate the D band in the DWCNTs, the final *R* value (0.04) is much lower than the values for 370, 375, and 400 °C. Analysis of panels b and c of Figure 6 leads us to the conclusion that, along with the amorphous species, smaller and defective tubes are oxidized, leading to the additional decrease in the D band area at 440 °C (Figure 6b) compared to that in the isothermal experiments at 370−400 °C. Please note that the lines for 350 and 365 °C can be superimposed and the curves obtained at 370, 375, and 400°C are almost identical. The significant increase in the G band intensity (Figure 6c) can be explained by the fact that the observed G band Raman signal comes mostly from tubes of a particular diameter range due to resonant effects. Thus oxidation of smaller tubes results in a higher percentage of resonance-enhanced nanotubes. Temperatures above 480 °C lead to the total oxidation of DWCNT samples, showing elimination of the D band and a time-dependent G band decrease. Figure 7 supports the observations of Figure

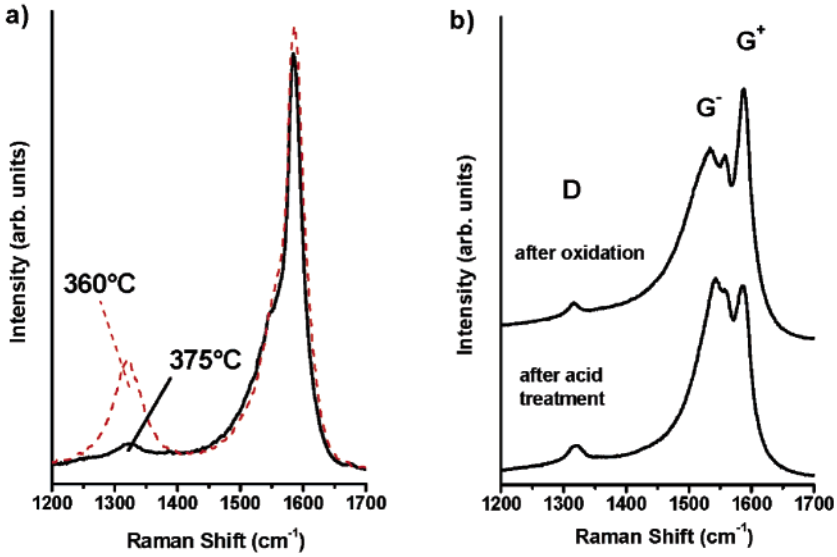

Figure 8. Raman spectra of: (a) DWCNTs after oxidation in a furnace at 360 °C (dashed line) and 375 °C (solid line). The *R* value decreases in the same way as that observed in the in situ experiments using the heating stage. The oxidation has also purified SWCNTs, leading to spectra similar to that of the acid-treated tubes. (b) Raman spectra of the SWCNTs after nonisothermal oxidation and washing in hydrochloric acid at room temperature for 24 h.

6. For temperatures between 350 and 370 °C, the RBM frequency ranges show similar shapes and intensity ratios between the peaks within the Raman spectrum, indicating that no nanotube structures are damaged or oxidized. Temperatures above 440 °C lead to some changes in the peak shape and intensity ratios of both the G band and RBM modes, induced by the oxidation of tubes with different diameters. The D band intensity shows no decrease for temperatures below 370 °C, whereas the decrease is similar for temperatures between 370 and 400 °C, where it reaches a final value of 65% of its original value. Above 440 °C, the final D band intensity, at the completion of the oxidation treatment, depends on the process temperature. Thus, the temperature range for the heating-induced purification of DWCNTs, with respect to the amorphous carbon, is between 370 and 400 °C. Furthermore, it is possible to develop an effective temperature-dependent oxidation method for nanotubes with different diameters and structural perfections.

Oxidation of larger amounts of DWCNTs using a furnace under similar conditions (Figure 8a) demonstrated the feasibility of scaling up the process. The furnace oxidation at 375 °C for 300 min showed a decrease in the *R* ratio similar to that after the heating stage experiments (Figure 8a). A similar furnace experiment, at 360 °C, showed no changes in the D band intensity or in *R*. Thus, the temperature range between 370 and 400 °C provides the optimal conditions for purification of the investigated DWCNTs.

Figure 8b shows the comparison between the SWCNTs oxidized in air and an acid-treated SWCNT sample.[28] The oxidation leads to a lower *R* value, which decreased from its original value of 0.07 to 0.02 after oxidation compared to an increase in value to 0.11 after the acid treatment. Thus, isothermal oxidation of carbon nanotubes is a promising method of purification with respect to the removal of nontubular carbon and defective tubes. Further experiments may identify isothermal oxidation methods that are specific not only to different carbon species but also to tube size and chirality.

Conclusions

In situ Raman spectroscopy analysis of the isothermal and nonisothermal oxidation of DWCNTs showed several common characteristics with the oxidation of SWCNTs. Temperature-induced shifts in the Raman spectrum of DWCNTs are between the values of those in SWCNTs and graphite. In situ Raman spectroscopy analysis of the oxidation of DWCNTs showed a decrease in the intensity of the D band starting around 370 °C, with complete D band elimination at 440 °C, with the decrease in the D band strongly dependent on the temperature. This suggests that the D band of DWCNTs is a combination of Raman signals originating from the amorphous carbon present in the sample and the defects in the tube walls. Controlled oxidation in air provides a method for removing disordered carbon and obtaining nanotube samples with a low *R* ratio or a negligible intensity of the D band. The oxidation of amorphous material is not accompanied by tube damage. A similar decrease in the D band intensity was also observed in SWCNTs but the D band was not completely eliminated.

Acknowledgment. The authors are thankful to Mr. K. Behler, Drexel University, for helpful comments on the paper. This work was supported in part by Arkema, France. E.F. thanks Dr. P. Puech for fruitful discussions. The experiments were performed using the centralized Materials Characterization Facility of the A. J. Drexel Nanotechnology Institute.

CM052755G